Electrical Control of Optical Plasmon Resonance with Graphene

Jonghwan Kim,[†] Hyungmok Son,[†] David J. Cho,[†,‡] Baisong Geng,[†] Will Regan,[†,‡] Sufei Shi,[†] Kwanpyo Kim,[†,‡] Alex Zettl,[†,‡] Yuen-Ron Shen,[†,‡] and Feng Wang*[,†,‡]

[†]Department of Physics, University of California at Berkeley, Berkeley, California 94720, United States
[‡]Materials Science Division, Lawrence Berkeley National Laboratory, Berkeley, California 94720, United States

ⓢ Supporting Information

ABSTRACT: Surface plasmon has the unique capability to concentrate light into subwavelength volume.[1−5] Active plasmon devices using electrostatic gating can enable flexible control of the plasmon excitations,[6] which has been demonstrated recently in terahertz plasmonic structures.[7−9] Controlling plasmon resonance at optical frequencies, however, remains a significant challenge because gate-induced free electrons have very weak responses at optical frequencies.[10] Here we achieve efficient control of near-infrared plasmon resonance in a hybrid graphene-gold nanorod system. Exploiting the uniquely strong[11,12] and gate-tunable optical transitions[13,14] of graphene, we are able to significantly modulate both the resonance frequency and quality factor of gold nanorod plasmon. Our analysis shows that the plasmon−graphene coupling is remarkably strong: even a single electron in graphene at the plasmonic hotspot could have an observable effect on plasmon scattering intensity. Such hybrid graphene−nanometallic structure provides a powerful way for electrical control of plasmon resonances at optical frequencies and could enable novel plasmonic sensing down to single charge transfer events.

KEYWORDS: Graphene, plasmon resonance, metamaterials, active plasmonics, gold nanorod, charge transfer sensor
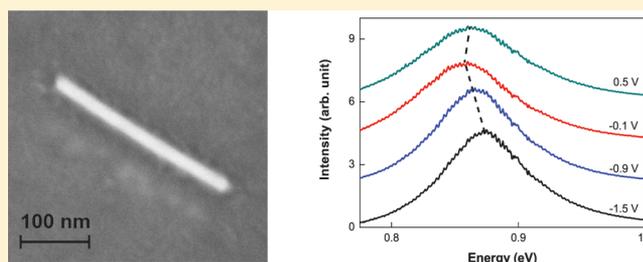
Surface plasmon resonance in nanoscale metal structures has attracted tremendous interest due to its unique capability to concentrate light into a deep subwavelength scale.[5] In applications ranging from nanoantenna[1] to metamaterials[3,4] it is often desirable to have plasmonic resonances that can be controlled in situ with electrostatic gating. So far, such active plasmonic devices have been demonstrated only at terahertz frequencies employing hybrid semiconductor−metal nanostructures,[7−9] because gate-induced free electrons in typical semiconductors have large responses only at this low-frequency range.[10] At optical frequencies (including near-infrared to visible), electrical control of plasmon resonance has been an outstanding challenge due to the dramatically reduced free electron responses with increasing frequency. Graphene, a novel zero-bandgap semiconductor,[15,16] provides a unique opportunity to address this challenge, because not only the low-frequency free carrier response but also the high-frequency interband transition in graphene can be conveniently varied through electrical gating.[13,14] In addition, graphene can be readily integrated into the nanometer-sized hot spot in the nanometallic structure due to its single atom thickness and excellent compatibility with nanofabrication.[17−19]

Here we demonstrate electrical controlled plasmonic resonance at near-infrared using the hybrid graphene-gold nanorod structure as a model system. This is in contrast to intrinsic graphene plasmonics that arises from free carriers at terahertz and far-infrared frequencies.[20−22] Such plasmon resonance control is also distinctly different from enhancing absorption for graphene photo detectors.[23,24] We show that, although graphene is only a single atom thick, its effect on the gold nanorod plasmon is remarkably strong: Electrical gating of graphene efficiently modulates all aspects of the plasmon resonance, including a 20 meV shift of resonance frequency, a 30% increase in quality factor, and a 30% increase in resonance scattering intensity. The plasmon resonance frequency shift and the resonance quality factor increase can be attributed to, respectively, changes in the real (ε_g') and imaginary (ε_g'') part of the graphene dielectric constant upon electrical gating. Our analysis further shows that surprisingly few graphene electrons at the plasmon hot spots contribute to a large fraction of the plasmon modulation, with each additional electron changing the plasmon scattering intensity by about one thousandth. This intensity change, we note, is well within the detection limit of modern photonic technology, and it could enable ultrasensitive optical detection of single charge transfer events. The hybrid graphene−nanometallic structure therefore opens up opportunities not only to active control near-infrared plasmon resonances, but also to novel single-electron sensing.

Figure 1a illustrates our device configuration, where graphene is placed on top of gold nanorods. Figure 1b shows

	Form Approved OMB No. 0704-0188
Report Documentation Page	*Form Approved* *OMB No. 0704-0188*

Public reporting burden for the collection of information is estimated to average 1 hour per response, including the time for reviewing instructions, searching existing data sources, gathering and maintaining the data needed, and completing and reviewing the collection of information. Send comments regarding this burden estimate or any other aspect of this collection of information, including suggestions for reducing this burden, to Washington Headquarters Services, Directorate for Information Operations and Reports, 1215 Jefferson Davis Highway, Suite 1204, Arlington VA 22202-4302. Respondents should be aware that notwithstanding any other provision of law, no person shall be subject to a penalty for failing to comply with a collection of information if it does not display a currently valid OMB control number.

1. REPORT DATE **01 OCT 2012**	2. REPORT TYPE	3. DATES COVERED **00-00-2012 to 00-00-2012**
4. TITLE AND SUBTITLE **Electrical Control of Optical Plasmon Resonance with Graphene**		5a. CONTRACT NUMBER
		5b. GRANT NUMBER
		5c. PROGRAM ELEMENT NUMBER
6. AUTHOR(S)		5d. PROJECT NUMBER
		5e. TASK NUMBER
		5f. WORK UNIT NUMBER
7. PERFORMING ORGANIZATION NAME(S) AND ADDRESS(ES) **University of California at Berkeley,Department of Physics,Berkeley,CA,94720**		8. PERFORMING ORGANIZATION REPORT NUMBER
9. SPONSORING/MONITORING AGENCY NAME(S) AND ADDRESS(ES)		10. SPONSOR/MONITOR'S ACRONYM(S)
		11. SPONSOR/MONITOR'S REPORT NUMBER(S)

12. DISTRIBUTION/AVAILABILITY STATEMENT
Approved for public release; distribution unlimited

13. SUPPLEMENTARY NOTES

14. ABSTRACT
Surface plasmon has the unique capability to concentrate light into subwavelength volume.1−5 Active plasmon devices using electrostatic gating can enable flexible control of the plasmon excitations,6 which has been demonstrated recently in terahertz plasmonic structures.7−9 Controlling plasmon resonance at optical frequencies however, remains a significant challenge because gate-induced free electrons have very weak responses at optical frequencies.10 Here we achieve efficient control of nearinfrared plasmon resonance in a hybrid graphene-gold nanorod system. Exploiting the uniquely strong11,12 and gate-tunable optical transitions13,14 of graphene, we are able to significantly modulate both the resonance frequency and quality factor of gold nanorod plasmon. Our analysis shows that the plasmon−graphene coupling is remarkably strong: even a single electron in graphene at the plasmonic hotspot could have an observable effect on plasmon scattering intensity. Such hybrid graphene−nanometallic structure provides a powerful way for electrical control of plasmon resonances at optical frequencies and could enable novel plasmonic sensing down to single charge transfer events.

15. SUBJECT TERMS

16. SECURITY CLASSIFICATION OF:			17. LIMITATION OF ABSTRACT	18. NUMBER OF PAGES	19a. NAME OF RESPONSIBLE PERSON
a. REPORT **unclassified**	b. ABSTRACT **unclassified**	c. THIS PAGE **unclassified**	**Same as Report (SAR)**	**5**	
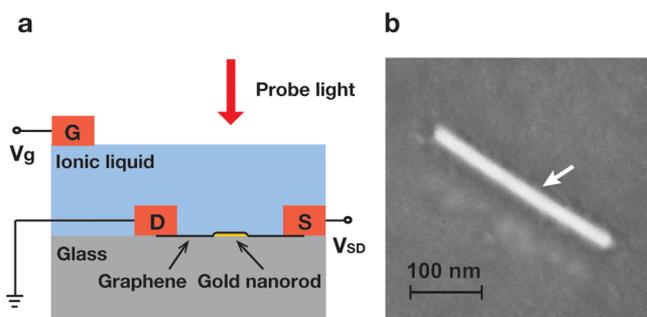
Figure 1. Graphene-gold nanorod hybrid structure. (a) Illustration of a typical device with graphene placed on top of gold nanorods. A top electrolyte gate with ionic liquid is used to control plasmon resonance through varying optical transitions in graphene. (b) A typical high-resolution scanning electron micrograph (SEM) of the single gold nanorod covered by graphene. Individual gold nanorods are well-separated from each other in our devices, and graphene is observed to drape nicely over the nanorods (white arrow).

a typical high-resolution scanning electron micrograph (SEM) of the single gold nanorod covered by graphene in our devices. We used top electrolyte gating with ionic liquid to control optical transitions in graphene.[25] The consequent changes in plasmon resonance of individual graphene−nanorod hybrid structures were probed with dark-field Rayleigh scattering spectroscopy.

Figure 2a and b display two representative single-particle Rayleigh scattering spectra of an ungated graphene−nanorod hybrid structure and a bare gold nanorod, respectively. Both scattering spectra exhibit prominent plasmon resonances at 0.86 eV (i.e., at the telecom wavelength of 1.5 μm). However, the plasmon resonance of the graphene-nanorod hybrid structure is much broader, with a full-width-half-maximum (fwhm), at 93 meV (compared to 70 meV in a bare gold nanorod). It is quite surprising that a monolayer thick graphene can lead to such a large change in plasmon resonances in the gold nanorod. This underlines remarkably strong interband optical absorption of graphene at in optical frequencies (Figure 2c),[11,12] which provides an efficient dissipation channel and increases the damping rate of the surface plasmon oscillation.[17,26]

To modulate the quality factor and scattering intensity of the plasmon resonance, one can simply eliminate the energy dissipation channel in graphene by switching off its interband optical transitions. This can be achieved through electrostatic gating: gated graphene has a shifted Fermi energy $|E_F|$, and optical transitions with energy less than $2|E_F|$ become forbidden due to empty initial states (or filled final states) for hole (or electron) doping (Figure 2d).[13,14] We can determine this gate-induced change in graphene absorption using infrared reflection spectroscopy. Figure 3a displays the gate-induced reflectivity change $\delta R/R$ at the plasmon resonance energy 0.86 eV in an area with only graphene. It shows a step-function-like decrease in reflectivity, corresponding to reduced graphene absorption,[12] at large hole doping (with V_g lower than −0.1 V). This gate-dependent reflectivity curve indicates that our as-prepared graphene under ionic liquid is strongly hole-doped, and $2|E_F|$ reaches the probe photon energy of 0.86 eV at V_g = −0.1 V. Similar curves obtained at different probe photon energies allow us to determine the $2|E_F|$ value of graphene at different applied gate voltages.
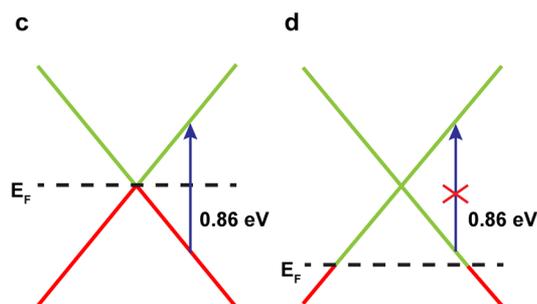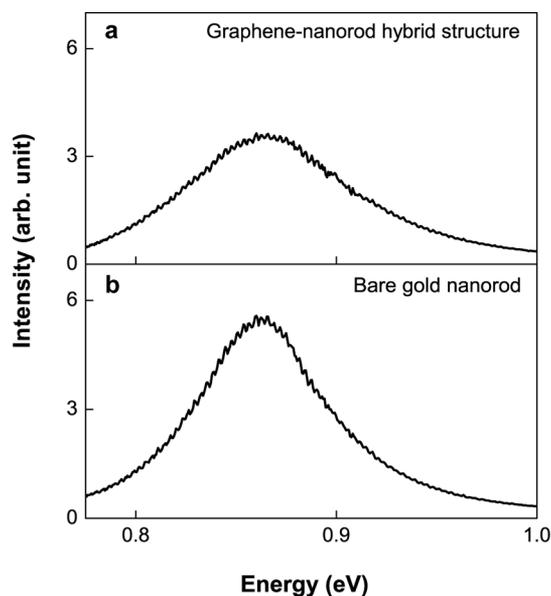
Figure 2. Effect of graphene on the gold nanorod plasmon resonance. (a) Rayleigh scattering spectra of an as-prepared graphene-nanorod hybrid structure. (b) Rayleigh scattering spectrum of a bare gold nanorod. Both scattering spectra exhibit prominent plasmon resonances at 0.86 eV (i.e., at the telecom wavelength of 1.5 μm), but the resonance in graphene-nanorod hybrid structure is significantly broader due to extra dissipation channel from graphene absorption. (c) Illustration of strong interband optical transitions present at all energies in pristine graphene. They contribute to the plasmon dissipation at 0.86 eV. (d) Illustration showing that a gate-induced shift in Fermi energy (E_F) can block the interband transition in graphene and reduce optical dissipation at 0.86 eV.

Rayleigh scattering intensity from an individual graphene−nanorod hybrid structure as a function of the photon energy and gate voltage is displayed in a two-dimensional (2D) color plot in Figure 3b. Figure 3c shows four line cuts of the 2D plot for Rayleigh scattering spectra at V_g = 0.5, −0.1, −0.9, and −1.5 V, which clearly demonstrate the capability to modulate surface plasmon resonance through electrical gating. The detailed dependences of plasmon resonance energy (E_R), width (Γ_R), and peak intensity (I_P) on graphene $2|E_F|$ are shown in Figure 4a−c (symbols). The resonance width in Figure 4b displays a step-like decrease, corresponding to an increase in quality factor, with increasing $2|E_F|$. This is a direct consequence of blocked graphene optical absorption in highly doped graphene, which leads to a reduced ε_g'' in graphene and lower loss. The increased quality factor naturally leads to a higher scattering intensity at the plasmon resonance, as shown in Figure 4c. The plasmon resonance frequency exhibits an unusual behavior (Figure 4a): it shifts to lower energy, and then to higher energy, with increased graphene doping. This behavior can be
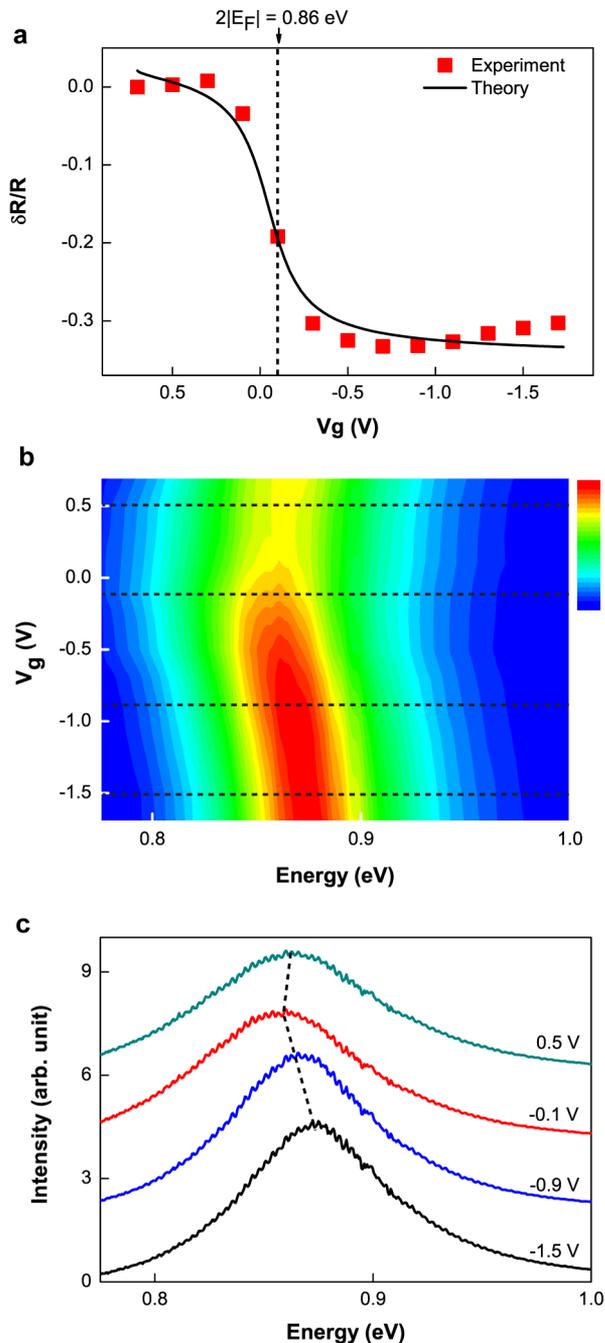
Figure 3. Electrical control of the plasmon resonance. (a) Gate-induced reflectivity change ($\delta R/R$) of graphene on the substrate probed at photon energy of 0.86 eV. It shows a step-function-like decrease in reflectivity, corresponding to a reduction of graphene absorption, due to blocked optical absorption at large hole doping (Figure 2d). The threshold voltage at $V_g = -0.1$ V is set by $2|E_F|$ reaching the probe photon energy of 0.86 eV. (It indicates that the as-prepared graphene under ionic liquid is strongly hole-doped.) (b) Scattering intensity (color scale, arbitrary units) is plotted as a function of the photon energy and gate voltage. (c) Rayleigh scattering spectra of an individual graphene−nanorod hybrid structure at $V_g = 0.5$, −0.1, −0.9, and −1.5 V, corresponding to the four horizontal (dashed) line cuts in b. Strong modulation of all aspects of the plasmon excitation, including the resonance frequency, quality factor, and scattering intensity, is achieved as electrostatic gating shifts the Fermi energy and modifies optical transitions in graphene.
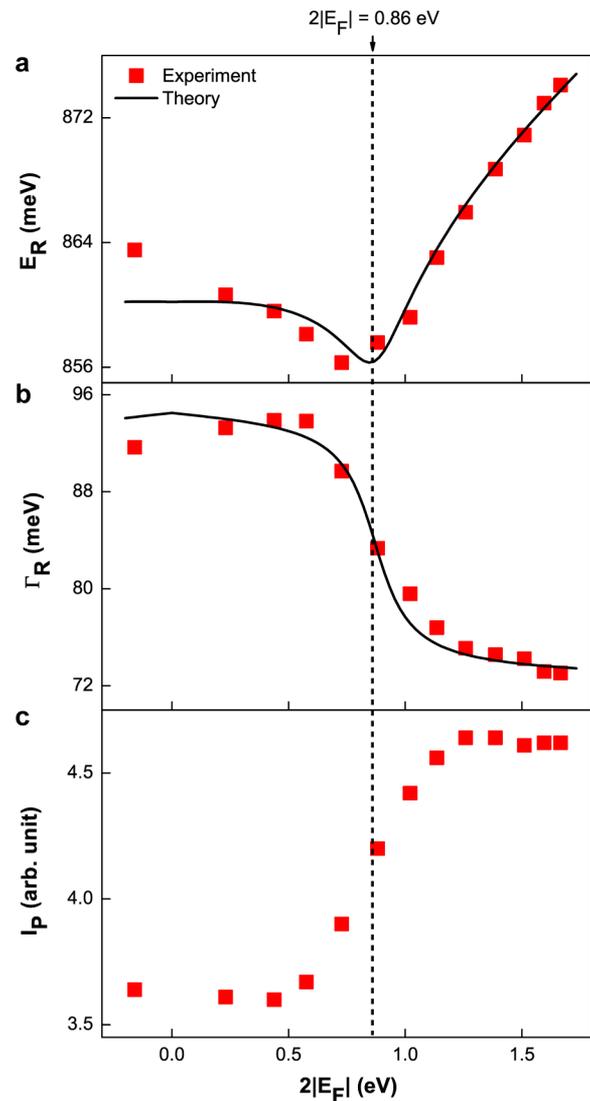
Figure 4. Comparison between experiment and theory. Symbols in a, b, and c show, respectively, detailed data of the plasmon resonance energy (E_R), width (Γ_R), and peak scattering intensity (I_P) as a function of $2|E_F|$ in graphene. Our model (solid line) reproduces nicely the experimental data, where the changes in the plasmon resonance energy and width originate from gate-induced modification in the real (ε'_g) and imaginary (ε''_g) part of graphene dielectric constant, respectively. The red and then blue shift of plasmon resonance frequency in a is due to an increase and then decrease of ε'_g in graphene at the plasmon resonance energy E_R when optical transitions change in graphene as doped. Intraband transition part provides monotonically decreasing contribution to ε'_g whereas the interband transition part provides a contribution which has maximum at $2|E_F| = E_R$. The decreased resonance width at large $2|E_F|$ in b is a consequence of reduced ε''_g and lower loss when optical transitions at E_R are blocked. This increased quality factor naturally leads to a higher scattering intensity at the plasmon resonance in c.

accounted for by gated-induced change in the real part of dielectric constant (ε'_g) of graphene, as we describe below.

Gate-dependent complex dielectric constant of graphene has been established previously.[12,27,28] The imaginary part ε''_g is characterized by a constant absorption of $(\pi e)^2/(\hbar c)$ above $2|E_F|$ from interband transitions and Drude absorption from free carriers (i.e., intraband transitions). The real part ε'_g can be

obtained from ε_g'' using the Kramer−Kronig relation. Specifically, energy-dependent ε_g' and ε_g'' have the form[27,28]

$$\varepsilon'_g(E) = 1 + \frac{e^2}{8\pi E \varepsilon_0 d} \ln \frac{(E + 2|E_F|)^2 + \Gamma^2}{(E - 2|E_F|)^2 + \Gamma^2}$$
$$- \frac{e^2}{\pi \varepsilon_0 d} \frac{|E_F|}{E^2 + (1/\tau)^2} \qquad (1)$$

$$\varepsilon''_g(E) = \frac{e^2}{4E\varepsilon_0 d}\left[1 + \frac{1}{\pi}\left\{\tan^{-1}\frac{E - 2|E_F|}{\Gamma}\right.\right.$$
$$\left.\left. - \tan^{-1}\frac{E + 2|E_F|}{\Gamma}\right\}\right] + \frac{e^2}{\pi\tau E\varepsilon_0 d}\frac{|E_F|}{E^2 + (1/\tau)^2}$$

Here d is the thickness of graphene. The interband transition broadening Γ is estimated to be 110 meV from the graphene reflection spectrum. The free carrier scattering rate $1/\tau$ can be set to zero because it has little effect on the dielectric constants, $\varepsilon_g'(E_R)$ and $\varepsilon_g''(E_R)$, at the plasmon resonance energy E_R. We have assumed that the interband transition broadening is dominated by finite lifetime of excited states and characterized by a Lorentzian line shape. Equation 1 shows that $\varepsilon_g''(E_R)$ experiences a step-like decrease when $2|E_F|$ is larger than E_R and blocks the relevant interband transitions. $\varepsilon_g'(E_R)$ has significant contribution both from intraband transition and interband transitions (see Supporting Information). The intraband transition contribution decreases monotonically with carrier doping. On the other hand, the interband transition contribution has a maximum at $2|E_F| = E_R$. This is because all optical transitions below E_R contribute a negative susceptibility, and transitions above E_R contribute a positive susceptibility to $\varepsilon_g'(E_R)$.

Figure 4a and b shows the relation between the changes in the plasmon resonance energy and width with the graphene dielectric constant ε_g' and ε_g''. We found that the frequency shift and width increase of the plasmon resonance scale linearly the gate-dependent ε_g' and ε_g'' of graphene, that is, $E_R = E_R^0 + \alpha\varepsilon_g'$ and $\Gamma_R = \Gamma_R^0 + \beta\varepsilon_g''$ (solid lines in Figure 4a and b). Here $E_R^0 = 862.4$ meV and $\Gamma_R^0 = 72.8$ meV are the plasmon resonance frequency and width for bare gold nanorod, and $\alpha = -3.693$ and $\beta = 4.828$ are two constant prefactors. (For best fitting we have also slightly shifted $|E_F|$ by 40 meV compared to the values we determined through optical spectroscopy at the region with only graphene. This shift is presumably due to slightly different carrier doping at the hot spot right next to gold.) Our simple model reproduces nicely the significant gate-induced decrease of plasmon resonance width (i.e., higher quality factor), as well as the red and blue shifts of the plasmon resonance energy. The increased scattering intensity arises naturally from the increased plasmon resonance quality factor.

Our numerical simulation further confirms the above picture. The simulation shows that electrical gating of graphene leads to a modulation of plasmon resonance quality factor by 28% (see Supporting Information), which agrees well with our experimental observation. Interestingly, a significant portion of this change arises from the hot spots at the two ends of the gold nanorods due to strongly enhanced electric field therein: Our simulation (Figure S2 in Supporting Information) shows that integrated intensity of the in-plane field within the hot spots (defined by two 20 nm × 20 nm area) constitutes 14% of integrated in-plane intensity overall the whole horizontal plane. It suggests that the small area of graphene at the hot spots 4%

increase in plasmon scattering intensity (i.e., 14% of total changes). This response arises from only ∼60 gate-induced electrons within the hot spot area given that a carrier concentration variation of $8 \times 10^{12}/\text{cm}^2$ is needed to shift the Fermi energy from 0.4 to 0.5 eV and block interband transition in graphene,[13,14] which can couple with the resonance-electric field of a gold nanorod. Therefore the addition of a single electron (or hole) at the plasmonic hot spot, such as from charge transfer, can modify resonance scattering intensity by about 0.07%. In comparison, the shot-noise limited detection sensitivity is about $10^{-6}/(\text{Hz})^{1/2}$ for nanorod plasmon scattering with focused 1 mW laser excitation (see Supporting Information). It suggests that even a single electron can have a potentially observable effect on gold nanorod plasmon scattering intensity. This extremely strong interaction between graphene and plasmon resonance can enable the detection of individual single charge transfer event at the plasmonic hot spot.

In conclusion, we demonstrate efficient electrical modulation of plasmon resonance at optical frequencies utilizing the strong and tunable interband transitions in graphene. It not only allows for in situ control of optical light at subwavelength scale but also offers new opportunities for single charge and molecular sensing. Our study also raises an interesting question: what is the optimal plasmonic structure for the maximized interaction between graphene and the plasmonic resonance? Such an optimized structure is likely to have much enhanced plasmon modulation based on electrical gating of graphene and will pave the way for new kinds of plasmonic applications.

Methods. Chemically synthesized gold nanorods were purchased from Nanopartz (part number: 30-HAR-1400). The gold nanorods have a mean diameter of 25 nm and length of 200 nm, with a plasmon resonance energy at 860 meV on glass substrates.[29] Gold nanorods were deposited on a glass or SiO_2/Si substrate by spin coating at a spinning speed of 500 rpm. The substrate with gold nanorods was then immersed in acetone at 70 °C for 30 min to dissolve residual cetrimonium bromide (CTAB). On top of the nanorods we transferred a large-area graphene grown by chemical vapor deposition using the standard growth and transfer processes.[30,31] For electro-static gating of graphene we used a top electrolyte gating with ionic liquid 1-ethyl-3-methylimidazolium bis-(trifluoromethylsulfonyl)imide (EMI-TFSI).[25] Figure 1b displays a typical high-resolution scanning electron micrograph (SEM) of the gold nanorod covered by graphene on SiO_2/Si substrate. Our SEM images show that the gold nanorods have a length distribution from 155 to 311 nm, and they form mostly well-separated individual rods in our devices. Transferred large area graphene draped nicely around the gold nanorods, as can be seen at the nanorod edges in the SEM image.

The electrically tunable plasmon resonance in the hybrid graphene-nanorod structure is probed using a dark-field Rayleigh scattering spectroscopy of individual gold nanorods. We used a supercontinuum laser as the broadband light source producing high brightness photons from 0.67 to 2.7 eV. The supercontinuum light is focused to excite gold nanorods in a microscopy setup. The Rayleigh scattering light from individual nanorods is collected using confocal microscopy in dark-field configuration and analyzed by a spectrometer equipped with an InGaAs array detector.

ASSOCIATED CONTENT

Ⓢ Supporting Information

Calculation on gate-dependent dielectric constants of graphene, finite element analysis on optical plasmon resonance modulation with graphene, estimation of shot-noise-limited detection. This material is available free of charge via the Internet at http://pubs.acs.org.

AUTHOR INFORMATION

Corresponding Author
*E-mail: fengwang76@berkeley.edu.

Notes
The authors declare no competing financial interest.

ACKNOWLEDGMENTS

REFERENCES

(1) Mühlschlegel, P.; Eisler, H.-J.; Martin, O. J. F.; Hecht, B.; Pohl, D. W. Resonant Optical Antennas. *Science* **2005**, *308*, 1607–1609.

(2) Nie, S.; Emory, S. R. Probing Single Molecules and Single Nanoparticles by Surface-Enhanced Raman Scattering. *Science* **1997**, *275*, 1102–1106.

(3) Lezec, H. J.; Dionne, J. A.; Atwater, H. A. Negative Refraction at Visible Frequencies. *Science* **2007**, *316*, 430–432.

(4) Valentine, J.; et al. Three-dimensional optical metamaterial with a negative refractive index. *Nature* **2008**, *455*, 376–379.

(5) Schuller, J. A.; et al. Plasmonics for extreme light concentration and manipulation. *Nat. Mater.* **2010**, *9*, 193–204.

(6) Dionne, J. A.; Diest, K.; Sweatlock, L. A.; Atwater, H. A. PlasMOStor: A Metal–Oxide–Si Field Effect Plasmonic Modulator. *Nano Lett.* **2009**, *9*, 897–902.

(7) Chen, H.-T.; et al. Active terahertz metamaterial devices. *Nature* **2006**, *444*, 597–600.

(8) Chen, H.-T.; et al. A metamaterial solid-state terahertz phase modulator. *Nat. Photon.* **2009**, *3*, 148–151.

(9) Chen, H.-T.; et al. Electronic control of extraordinary terahertz transmission throughsubwavelength metal hole arrays. *Opt. Express* **2008**, *16*, 7641–7648.

(10) Yu, P. Y.; Cardona, M. *Fundamentals of Semiconductors*; Springer: New York, 2004; p 305.

(11) Nair, R. R.; et al. Fine Structure Constant Defines Visual Transparency of Graphene. *Science* **2008**, *320*, 1308.

(12) Mak, K. F.; et al. Measurement of the Optical Conductivity of Graphene. *Phys. Rev. Lett.* **2008**, *101*, 196405.

(13) Li, Z. Q.; et al. Dirac charge dynamics in graphene by infrared spectroscopy. *Nat. Phys.* **2008**, *4*, 532–535.

(14) Wang, F.; et al. Gate-Variable Optical Transitions in Graphene. *Science* **2008**, *320*, 206–209.

(15) Novoselov, K. S.; et al. Two-dimensional gas of massless Dirac fermions in graphene. *Nature* **2005**, *438*, 197–200.

(16) Zhang, Y.; Tan, Y.-W.; Stormer, H. L.; Kim, P. Experimental observation of the quantum Hall effect and Berry's phase in graphene. *Nature* **2005**, *438*, 201–204.

(17) Papasimakis, N.; et al. Graphene in a photonic metamaterial. *Opt. Express* **2010**, *18*, 8353–8359.

(18) Liu, M.; et al. A graphene-based broadband optical modulator. *Nature* **2011**, *474*, 64–67.

(19) Xia, F.; Mueller, T.; Lin, Y.-m.; Valdes-Garcia, A.; Avouris, P. Ultrafast graphene photodetector. *Nat. Nano* **2009**, *4*, 839–843.

(20) Ju, L.; et al. Graphene plasmonics for tunable terahertz metamaterials. *Nat. Nano* **2011**, *6*, 630–634.

(21) Yan, H.; et al. Tunable infrared plasmonic devices using graphene/insulator stacks. *Nat. Nano* **2012**, *7*, 330–334.

(22) Fei, Z. et al. Gate-tuning of graphene plasmons revealed by infrared nano-imaging. *ArXiv:1202.4993v2*, **2012**.

(23) Echtermeyer, T. J.; et al. Strong plasmonic enhancement of photovoltage in graphene. *Nat. Commun.* **2011**, *2*, 458.

(24) Liu, Y.; et al. Plasmon resonance enhanced multicolour photodetection by graphene. *Nat. Commun.* **2011**, *2*, 579.

(25) Chen, F.; Qing, Q.; Xia, J.; Li, J.; Tao, N. Electrochemical Gate-Controlled Charge Transport in Graphene in Ionic Liquid and Aqueous Solution. *J. Am. Chem. Soc.* **2009**, *131*, 9908–9909.

(26) Zou, Y.; Tassin, P.; Koschny, T.; Soukoulis, C. M. Interaction between graphene and metamaterials: split rings vs. wire pairs. *Opt. Express* **2012**, *20*, 12198–12204.

(27) Dawlaty, J. M.; et al. Measurement of the optical absorption spectra of epitaxial graphene from terahertz to visible. *Appl. Phys. Lett.* **2008**, *93*, 131905.

(28) Gusynin, V. P.; Sharapov, S. G.; Carbotte, J. P. Sum rules for the optical and Hall conductivity in graphene. *Phys. Rev. B* **2007**, *75*, 165407.

(29) Link, S.; El-Sayed, M. A. Spectral Properties and Relaxation Dynamics of Surface Plasmon Electronic Oscillations in Gold and Silver Nanodots and Nanorods. *J. Phys. Chem. B* **1999**, *103*, 8410–8426.

(30) Kim, K. S.; et al. Large-scale pattern growth of graphene films for stretchable transparent electrodes. *Nature* **2009**, *457*, 706–710.

(31) Li, X.; et al. Large-Area Synthesis of High-Quality and Uniform Graphene Films on Copper Foils. *Science* **2009**, *324*, 1312–1314.